

# Design and Analysis of Wind Turbine Systems with Open-Circuit Fault-Tolerant Control for Outer Switches of Five-Level Rectifiers

S.Bala Sai & P.Dhana Selvi

<sup>1</sup>PG Scholar, Dept of EEE, N.B.K.R.I.S.T, Vidyanagar, SPSR Nellore, AP, India, Email: balu85.bs@gmail.com

<sup>2</sup>Assistant professor, Dept of EEE, N.B.K.R.I.S.T, Vidyanagar, SPSR Nellore, AP, India,  
Email: [ghanaselvi.nbkrist@gmail.com](mailto:ghanaselvi.nbkrist@gmail.com)

**ABSTRACT-** This paper proposes a tolerant control for the open-circuit fault of the outer switches in three-level rectifiers (both 5L-NPC and T-type topologies) used in wind turbine systems. In this paper we increase the levels of NPC inverter if we increase the levels of inverter voltage level will be increased and thd will be reduced. A five-level converter is used as the power converters of wind turbine systems because of their advantages such as low-current total harmonic distortion, high efficiency, and low collector-emitter voltage. Interior permanent magnet synchronous generators (IPMSGs) have been chosen as the generator in wind turbine systems owing to their advantages of size and efficiency. In wind turbine systems consisting of the three-level converter and the IPMSG, fault-tolerant controls for an open-circuit fault of switches should be implemented to improve reliability. This paper focuses on the open-circuit fault of outer switches ( $S_{x1}$  and  $S_{x4}$ ) in three level rectifiers (both neutral-point clamped and T-type) that are connected to the IPMSG. In addition, the effects of  $S_{x1}$  and  $S_{x4}$  open-circuit faults are analyzed, and based on this analysis, a tolerant control is proposed. The proposed tolerant control maintains normal operation with sinusoidal currents under the open-circuit fault of outer switches by adding a compensation value to the reference voltages. By using the simulation results we can analyze the effectiveness and performance of the proposed tolerant control method.

## I. INTRODUCTION

Multi-level Inverters have found successful applications in medium voltage high-power electrical drives, such as mining, pumps, fans and tractions five-level topologies are widely used in back-to-back converters of wind turbine generation (WTG) systems. In comparison with a conventional two-level topology, five-level topologies have more advantages, particularly for the high power. Neutral-point clamped (NPC) and T-type are typical three-level topologies. The power capacity of a wind turbine system has been increasing consistently, leading to the development of generators with large power capacity [1]–[3]. There are many types of generators. Permanent magnet synchronous generators (PMSGs) have high efficiency and high reliability compared with induction generators. Generators requiring high voltage need to use multilevel converter topologies to reduce the collector-emitter voltage per switch. Among multilevel topologies, three-level topologies such as

the five-level neutral-point clamped (5L-NPC) and T-type topologies are applied in wind turbine systems with a wide power range. The five-level topology can easily be expanded from a two-level topology and is also easier to control compared with other multilevel topologies.

Furthermore, the three-level topology guarantees high efficiency and low-current total harmonic distortion (THD) in comparison with the two level topology [8]–[11]. The 5L-NPC topology is vulnerable to switch faults because many switches are used. Switch fault detection and tolerant control methods for switch faults should be implemented to improve the reliability of wind turbine systems. Switch faults are divided into a short-circuit fault In wind turbine systems, a back-to-back converter is used to transfer power from the generator to the grid. A back-to-back converter using the 5L-NPC topology is shown in Fig. 1.

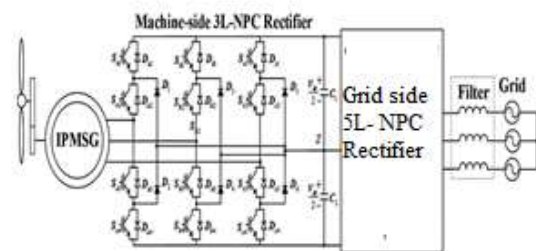


Fig. 1. Back-to-back converter using the 5L-NPC topology in wind turbine systems.

This consists of the machine-side 5L-NPC rectifier, the dc-link, and the grid-side 5L-NPC inverter. In the 5L-NPC inverter, the open-circuit fault of the inner switch causes the outer switch connected it to be infeasible; therefore, changing only the switching method does not become a solution for the open-circuit fault, and the additional devices such as fuses and switches should be added for achieving the tolerant operation under the open-circuit fault of the inner switch [16]–[18].

The tolerant control method limits the output voltage range by half. In the 5L-NPC rectifier, the current distortion caused by the open-circuit fault of the inner switch can be restored

partially by clamping the switching state without any additional devices [14]. In addition, the reactive current is injected to eliminate current distortion caused by the open-circuit fault of the outer switch [22]. This method can also be applied for the T-type rectifier. The T-type rectifier is advantageous on the tolerant control because the switches in a leg are independent of each other.

This paper focuses on the open-circuit fault of the machine side 5L-NPC rectifier. In general, the input currents of the 5L-NPC rectifier do not flow through the outer switches (Sx1 and Sx4) at unity power factor (pf); therefore, the existing tolerant controls for the 5L-NPC rectifier take into account only the inner switches (Sx2 and Sx3) [13]. However, according to the specification of the PMSG, an open-circuit fault of the outer switch can cause current distortion as much as when an open circuit fault of the inner switch occurs [22]. The tolerant control for Sx1 and Sx4 open-circuit faults are also proposed in [22], and this control method injects the exact reactive current required to eliminate the current distortion. This means that the pfs changed. Rectifiers with IPMSGs can operate to generate maximum power at pfs other than unity. IPMSGs provide more power

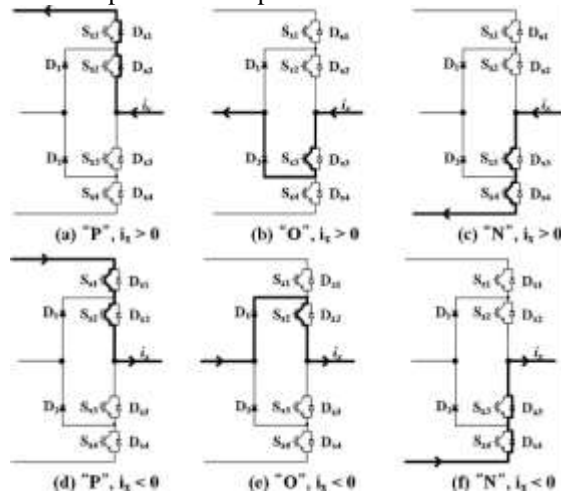


Fig. 2. Current paths depending on the current direction and the switching state.

When rectifiers operate at a unique-pf [4]–[7]. In such a case, an open-circuit fault of the outer switches (Sx1 and Sx4) causes current distortion and torque fluctuation, which can lead to vibration of the wind turbine. In this paper, the reason for the current distortion caused by the outer switches (Sx1 and Sx4) is analyzed, and then, on the basis of this analysis, a tolerant control for Sx1 and Sx4 open-circuit faults is proposed. In the proposed tolerant control, the switch with an open-circuit fault is not used to generate the input voltages of the three-level rectifier by adding a compensation value to the reference voltages. The compensation value is

simply calculated and the pf does not change in the proposed tolerant control. The performance of the proposed tolerance control is proved by simulation results.

### III. OPEN-CIRCUIT FAULT ANALYSIS OF OUTER SWITCHES

There are three switching states (P, N, and O) in the 5L-NPC rectifier [9]. Six current paths can be generated depending on the current direction and the switching state, and these are shown in Fig. 2 [23]. Fig. 3 shows the input current generation process of a rectifier with unity pf. The rectifier current is  $I_{rec}$ , the rectifier voltage is  $V_{rec}$ , and the back electromotive force (EMF) is  $V_{EMF}$ .

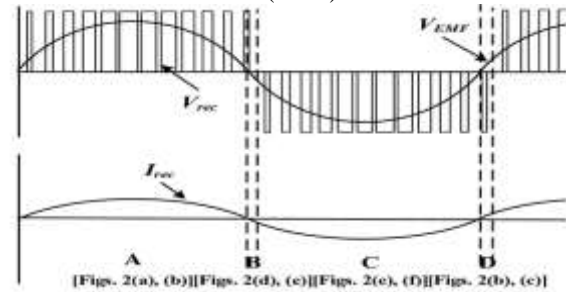


Fig. 3. Rectifier operation at unity pf.

TABLE I  
CURRENT PATH COMPOSITION DEPENDING ON THE PART OF FIG.3

Part	$V_{rec}$	$I_{rec}$	Current path
A	Positive	Positive	(a) P switching state, (b) O switching state (valid)
B	Positive	Negative	(d) P switching state (valid), (e) O switching state
C	Negative	Negative	(e) O switching state (valid), (f) N switching state
D	Negative	Positive	(b) O switching state, (c) N switching state (valid)

The phase difference between  $V_{EMF}$  and  $V_{rec}$ , which causes the current flow, is controlled to match the phase of  $I_{rec}$  up with the phase of the corresponding  $V_{EMF}$ . One period of  $I_{rec}$  can be divided into four parts depending on the polarity of  $I_{rec}$  and  $V_{rec}$ . The generated current paths are different depending on the part, and these are summarized in Table I. In parts A and C, the O switching state causes the input current flow; therefore, this is called the valid switching state. The current continuously flows through two diodes if the switching state is changed to P or N switching state in which no current flows through the switches.

In this paper, the other case (Case II), which is the reactive current injection for IPMSG, is also considered. Fig. 4 shows that the input current generation processes of the rectifier for Cases I and II.

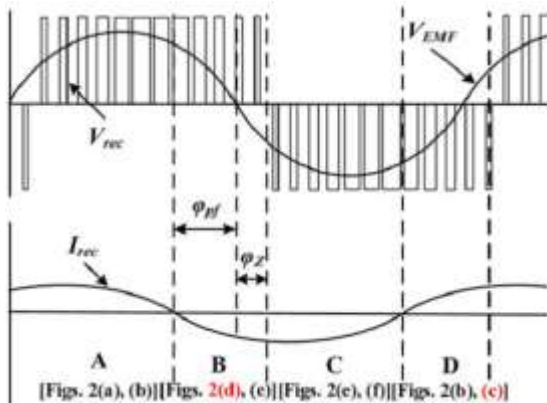


Fig. 4. Rectifier operation at any pf.

There are two phase differences: the phase difference ( $\phi_z$ ) between VEMF and  $V_{rec}$  explained in [22], and the phase difference ( $\phi_{pf}$ ) between  $I_{rec}$  and VEMF caused by the pf. In Fig. 4, part B (or part D) consists of  $\phi_z$  and  $\phi_{pf}$ , and their lengths increase. This means that the current can be more distorted by the open-circuit fault of the outer switches compared to when  $\phi_z$  alone is considered

Case I can be ignored because  $\phi_z$  is determined depending on the operating condition of the rectifier and the PMSG. However, because  $\phi_{pf}$  is determined by the pf, Case II should be considered when the IPMSG is employed. The current distortion caused by the open-circuit fault of the outer switches is shown in Fig. 5 for various pfs. Owing to the infeasible open-circuit fault switch, the current becomes zero during the range consisting of  $\phi_z$  and  $\phi_{pf}$ . The Sx1 open-circuit fault makes the current path of Fig. 2(d) infeasible.

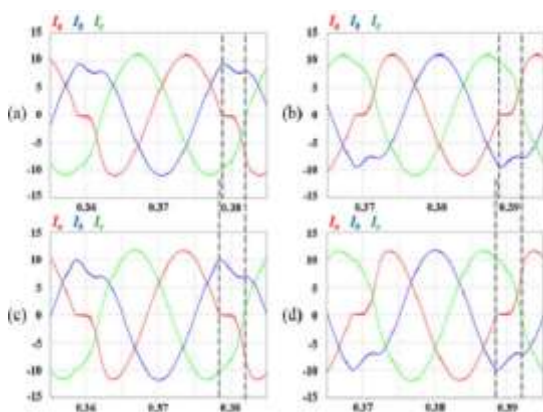


Fig. 5. Current distortion depending on the open-circuit fault and the pf: (a) 0.95pf, Sx1 open-circuit fault, (b) 0.95pf, Sx4 open-circuit fault, (c) 0.9pf, Sx1 open-circuit fault, and (d) 0.9pf, Sx4 open-circuit fault

The current path of Fig. 2(d) belongs to part B; therefore, the Sx1 open circuit fault causes

distortion in the negative current as shown in Fig. 5(a) and (c). On the contrary, the Sx4 open-circuit fault leads to distortion in the positive current as shown in Fig. 5(b) and (d) because the current path of Fig. 2(c) related to the Sx4 open-circuit fault belongs to part D. The low pf has a large  $\phi_{pf}$ . Therefore, the rectifier operation at a low pf leads to a large zero-current range when the open circuit fault of the outer switch occurs. As a result, the zero current range increases, as the pf decreases.

The analysis related to the open-circuit fault of the outer switches can be applied to the T-type topology. The effects of open-circuit faults of the outer switches on the current are the same in both the NPC rectifier and the T-type rectifier [13], [22]. Therefore, the current distortion caused by open-circuit faults of the outer switches in the NPC rectifier is the same as that in the T-type rectifier.

### III. TOLERANT CONTROL FOR OPEN-CIRCUIT FAULT OF OUTERS SWITCHES

An existing tolerant control method for the open-circuit fault of the outer switches is reactive current injection [22]. This method changes the phase of  $I_{rec}$  so that it corresponds with the phase of  $V_{rec}$ . This means that parts B and D are eliminated. However, this tolerant control method has the disadvantage of low-power generation efficiency of the generator because the PMSG has efficient operating condition which depends on the pf of the rectifier. In general, the unity pf is required for the best operating condition of a surface PMSG. The best operating condition of an IPMSG does not correspond to the unity pf, and this is determined by the specifications of the IPMSG. The proposed tolerant control does not change the pf of the rectifier. The rectifier voltage ( $V_{rec}$ ) without the current path related to the open-circuit fault switch is generated by changing the reference voltages. To explain the proposed tolerant control, the Sx1 open-circuit fault is used as an example.

#### A. Compensation Voltage ( $V_{comp}$ ) Calculation

Three-phase reference voltages ( $V_{x,ref}$ ,  $x=a, b, c$ ) are expressed as

$$V_{a,ref} = V_{mag} \cos \cos (2\pi f_s t)$$

$$V_{b,ref} = V_{mag} \cos \cos \left( 2\pi f_s t - \frac{2\pi}{3} \right)$$

$$V_{c,ref} = V_{mag} \cos \cos \left( 2\pi f_s t + \frac{2\pi}{3} \right) \quad (1)$$

Where  $V_{mag}$  is the magnitude of the reference voltages, and  $f_s$  is the fundamental frequency. The offset voltage ( $V_{offset}$ ) is added to each reference voltage to expand the range of the modulation index ( $M_a = \sqrt{3} \times V_{mag}/V_{dc}$ ).  $V_{offset}$  and the changed reference voltages ( $V_{x,ref,offset=a}$ ,  $b, c$ ) are expressed as

$$V_{offset} = -(V_{ref,max} + V_{ref,min})/2$$

$$V_{a,offset} = V_{a,ref} + V_{offset}$$

$$V_{b,offset} = V_{b,ref} + V_{offset} \quad (2)$$

$$V_{c,offset} = V_{c,ref} + V_{offset} \quad (3)$$

Where  $V_{ref,max}$  and  $V_{ref,min}$  are the maximum and minimum values of  $V_{a,ref}$ ,  $V_{b,ref}$ , and  $V_{c,ref}$ . The reference voltages of (3) are compared with the carrier signals to generate  $V_{rec}$ . When the  $S_{x1}$  open-circuit fault occurs, the current path of Fig. 2(d) should be eliminated to prevent current distortion; therefore, the reference voltage should be changed to generate  $V_{rec}$  without the current path of Fig. 2(d). In the proposed tolerant control, a reference voltage of a phase containing the  $S_x$  Open-circuit fault is changed to zero as shown in Fig. 6. As a result, the current path of Fig. 2(d) disappears because the O switching state is only used in part B. To make the reference voltage zero,  $|V_{comp}|$  is assigned the magnitude of the reference voltage ( $V_{x,ref,offset}$ ) containing the open-circuit fault, and  $V_{comp}$  can be expressed as

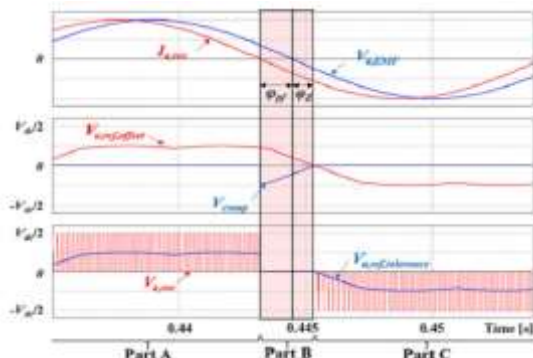


Fig. 6. Change of reference voltages in the proposed tolerant control for the  $S_{x1}$  open-circuit fault (0.95pf).

$$V_{comp} = -V_{x,ref,offset} \text{ (x=phase containing open - circuited fault switch)} \quad (4)$$

The proposed tolerant control is implemented by adding  $V_{comp}$  to the reference voltages ( $V_{x,ref,offset}$ ,  $x=a, b, c$ ). The new reference voltages ( $V_{x,ref,tolerance}$ ,  $x=a, b, c$ ) of the proposed tolerant control are expressed as

$$V_{a,ref,tolerance} = V_{a,ref,offset} + V_{comp}$$

$$V_{b,ref,tolerance} = V_{b,ref,offset} + V_{comp}$$

$$V_{c,ref,tolerance} = V_{c,ref,offset} + V_{comp} \quad (5)$$

### B. Compensation Range for Adding $V_{comp}$

By adding  $V_{comp}$  to each reference voltage, the use of the current path related to the open-circuit fault switch will be precluded. To achieve this perfectly,  $V_{comp}$  is added for the

suitable range and position. The compensation range, which is part B or part D of Fig. 4, consists of  $\phi_Z$ .  $\phi_Z$  can be calculated with the equivalent circuit of the PMSG and the three-level rectifier [22].  $\phi_Z$ , which is the phase difference between VEMF and  $V_{rec}$ , is expressed as

$$\phi_Z = \left( \frac{-|I_{rec}| * 2\pi f_s L}{V_{EMF} - |I_{ref}| R} \right) \quad (6)$$

Where  $R$  and  $L$  are the equivalent resistance and inductance of the PMSG, and  $f_s$  is the fundamental frequency representing the angular frequency of the PMSG.  $\phi_{pf}$ , which is the phase difference between VEMF and  $I_{rec}$ , is related to the  $\phi$ .  $\phi_{pf}$  can be calculated by the  $\phi$  and this is

TABLE II  
COMPENSATION RANGE DEPENDING ON THE POSITION OF THE OPEN-CIRCUIT FAULT

Position of open-circuit fault	Compensation range
$S_{a1}$	$(0^\circ - \phi_{pf}) \sim (0^\circ + \phi_Z)$
$S_{c4}$	$(60^\circ - \phi_{pf}) \sim (60^\circ + \phi_Z)$
$S_{b1}$	$(120^\circ - \phi_{pf}) \sim (120^\circ + \phi_Z)$
$S_{a4}$	$(180^\circ - \phi_{pf}) \sim (180^\circ + \phi_Z)$
$S_{c1}$	$(240^\circ - \phi_{pf}) \sim (240^\circ + \phi_Z)$
$S_{b4}$	$(300^\circ - \phi_{pf}) \sim (300^\circ + \phi_Z)$

expressed as

$$\phi_{pf} = (pf) \quad (7)$$

If the d-q control theorem is used,  $\phi_{pf}$  can be calculated as

$$\phi_{pf} = \left( \frac{I_{qe}}{\sqrt{I_{qe}^2 + I_{de}^2}} \right) \quad (8)$$

Where  $I_{de}$  indicates the d-axis current related to the flux and  $I_{qe}$  indicates the q-axis current related to the torque, and these are values in the d-q synchronous rotating frame.  $\phi_Z$  and  $\phi_{pf}$ , which are calculated from (6) and (8), are located near the zero-crossing point of VEMF as shown in Fig. 6. Therefore, the compensation position for adding  $V_{comp}$  is defined on the basis of VEMF's angle ( $\theta_{EMF}$ ). Fig. 7 shows three-phase VEMFs and  $\theta_{EMF}$ .  $\theta_{EMF}$  is acquired from the encoder or position sensor. Six zero-crossing points are expressed for every  $60^\circ$ , which are matched to each open-circuit fault as shown in Fig. 7.

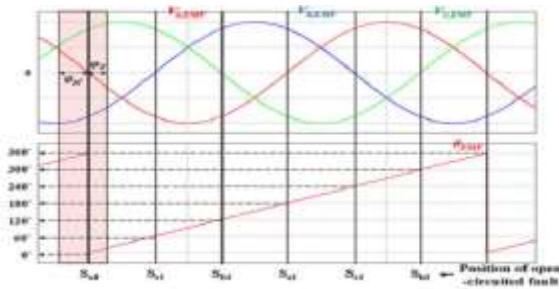


Fig. 7. Compensation position on the basis of VEMF's angle ( $\theta_{EMF}$ ).

Consequently,  $\theta_{EMF}$  representing each zero-crossing point is a criterion for adding  $V_{comp}$ . For example, when the  $S_{a1}$  open circuit fault occurs,  $V_{comp}$  should be added for the compensation range from  $(0^\circ - \phi_{pf})$  to  $(0^\circ + \phi_Z)$  which is based on  $0^\circ$ . By considering all open-circuit faults, Table II shows the compensation ranges for eliminating the current distortion depending on the position of the open-circuit fault

**C. Considering Neutral-Point Voltage Balance**

The compensation voltage which is one of the offset voltages can cause neutral-point voltage unbalance because  $V_{comp}$  calculated from (4) is a one-sided voltage [10], [24]. Therefore, two dc-link capacitors have different values depending on the polarity of  $V_{comp}$  generated for the open-circuit fault.

Fig. 8 shows the concept of proposed tolerant control considering the neutral-point voltage balance when the  $S_{a1}$  open-circuit fault occurs.

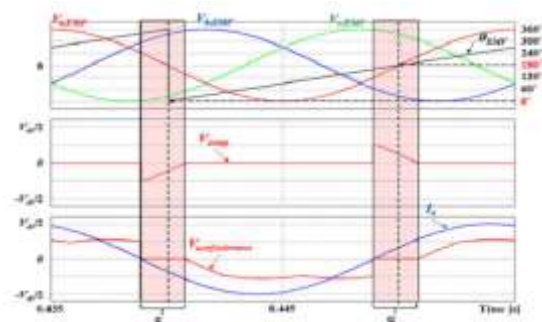


Fig. 8. Proposed tolerant control considering neutral-point voltage balance under the  $S_{a1}$  open-circuit fault.

In Fig. 8,  $V_{comp}$  is added for the compensation range  $[(0^\circ - \phi_{pf}) \sim (0^\circ + \phi_Z)]$  which corresponds to the position for the  $S_{a1}$  open-circuit fault; in addition,  $V_{comp}$  is also added for the diametrically opposite compensation range  $[(180^\circ - \phi_{pf}) \sim (180^\circ + \phi_Z)]$ , which is the range for the  $S_{a4}$  open-circuit fault. The final principles of the proposed tolerant control with the neutral-point voltage balance are summarized in Table III.

TABLE III

PRINCIPLE OF THE PROPOSED TOLERANT CONTROL DEPENDING ON THE POSITION OF THE OPEN-CIRCUIT FAULT

Position of open-circuit fault	$V_{comp}$	Compensation range
$S_{a1}$ or $S_{a4}$	$-V_{a,ref,offset}$	$(0^\circ - \phi_{pf}) \sim (0^\circ + \phi_Z)$
$S_{c1}$ or $S_{c4}$	$-V_{c,ref,offset}$	$(60^\circ - \phi_{pf}) \sim (60^\circ + \phi_Z)$
$S_{b1}$ or $S_{b4}$	$-V_{b,ref,offset}$	$(120^\circ - \phi_{pf}) \sim (120^\circ + \phi_Z)$
$S_{a4}$ or $S_{a1}$	$-V_{a,ref,offset}$	$(180^\circ - \phi_{pf}) \sim (180^\circ + \phi_Z)$
$S_{c4}$ or $S_{c1}$	$-V_{c,ref,offset}$	$(240^\circ - \phi_{pf}) \sim (240^\circ + \phi_Z)$
$S_{b4}$ or $S_{b1}$	$-V_{b,ref,offset}$	$(300^\circ - \phi_{pf}) \sim (300^\circ + \phi_Z)$

**D. Limitation of Proposed Tolerant Control**

$V_{x,ref,tolerance}$  cannot exceed a limitation voltage ( $V_{limit}$ ) which is restricted by the dc-link voltage ( $V_{dc}$ ). Therefore,  $V_{comp}$  is limited as follows

$$V_{comp} < V_{limit} - V_{ref,max} \tag{9}$$

Where  $V_{limit}$  is  $V_{dc}/2$ . On the basis of (9), the applicable operation range of the proposed tolerant control is determined depending on  $M_a$  and the pf. Fig. 9 shows  $V_{x,ref,tolerance}$  and  $V_{comp}$  of the proposed tolerant control depending on the pf when  $M_a$  is 0.5.

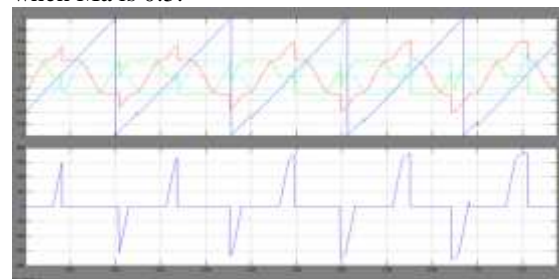


Fig. 9.  $V_{x,ref,tolerance}$  ( $x=a,b,c$ ) and  $V_{comp}$  depending on the pf when  $M_a$  is 0.5.

Fig. 10 shows the applicable pf range for various values of  $M_a$ . The shaded part of Fig. 10 represents the applicable operation range.

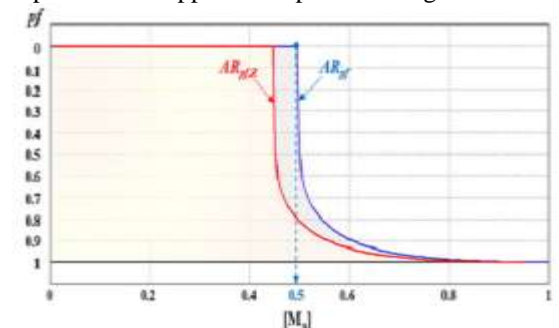


Fig. 10. Applicable pf range of the proposed tolerant control depending on  $M_a$ .

The proposed tolerant control is feasible over the entire factor range when  $M_a$  is smaller than

0.5. By increasing Ma from 0.5, the applicable operation range decreases. In Fig 10.

TABLE IV  
IPMSG PARAMETERS INSIMULATION

Rated power	2.5 MW
Number of pole	8
Rated voltage (line-to-line)	760 V <sub>rms</sub>
Rated current	1902 A <sub>rms</sub>
Rated speed	1650 rpm
Resistance	0.4567 mΩ
q-inductance	0.0982 mH
d-inductance	0.0725 mH

The proposed tolerant control has a limitation on its operation range that depends on the pf and Ma. However, considering that wind turbine systems do not always operate with the rated wind speed (high Ma) and that the operating pf of the rectifier with an IPMSG is not too low, the proposed tolerant control can clearly be effective

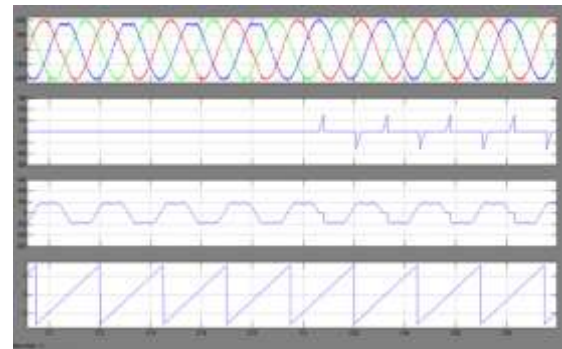
IV. SIMULATION RESULTS

The simulation is performed using the PSIM tool. The 5L-NPC rectifier of the back-to-back converter with 2.5-MW IPMSG is only considered in the simulation. The IPMSG parameters used in the simulation are shown in Table V.

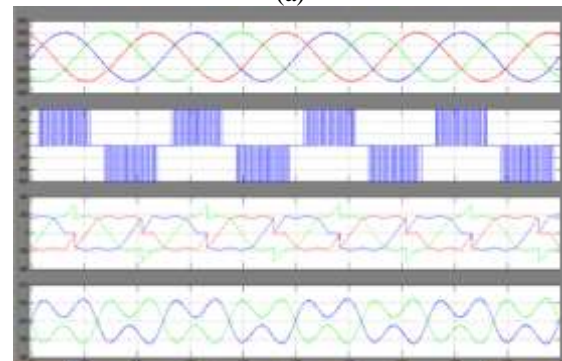
TABLE V  
IPMSG PARAMETERS

Rated power	11 kW
Number of pole	6
Rated voltage (line-to-line)	380 V <sub>rms</sub>
Rated current	19.9 A <sub>rms</sub>
Rated speed	1750 rpm
Resistance	0.349 Ω
q-inductance	15.6 mH
d-inductance	13.16 mH

After the proposed tolerant control is applied, the reference voltages are changed by V<sub>comp</sub> for the corresponding ranges[(0 °-φpf)~(0 °+φZ),(180 °-φpf)~(180 °+φZ)] which are defined in Table III. As a result, the a-phase pole voltage (V<sub>an</sub>) is clamped to 0 at their ranges as shown in Fig. 11(b) and the current distortion is eliminated completely.



(a)



(b)

Fig. 11. Simulation results with the proposed tolerant control under the Sa1 open-circuit fault (600 rpm, Ma =0.35, 0.95pf).

In addition, the two dc-link capacitor voltages are balanced. The proposed tolerant control is effective for the pf transition operation of the rectifier. Fig. 12 shows the results when the proposed tolerant control is applied and the pf is changed from 0.95 to 0.9.

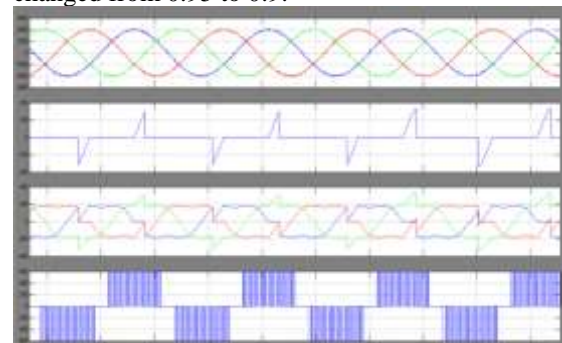


Fig. 12. Simulation results with the proposed tolerant control under the Sa1 open-circuit fault (600 rpm, Ma =0.35, pf-transition from 0.95 to 0.9).

Fig. 13 shows the performance of the proposed tolerant control under the Sa1 open-circuit fault at different speed (1000 rpm) of the PMSG when Ma is 0.59. Similar to Fig. 11, the distorted currents are corrected after the proposed tolerant control is applied.

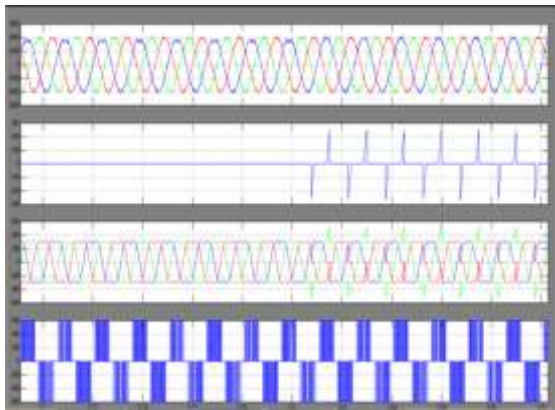


Fig. 13. Simulation results with the proposed tolerant control under the  $S_{a1}$  open-circuit fault (1000 rpm,  $M_a = 0.59, 0.95\text{pf}$ )

Table IV shows the current THD results before and after the proposed tolerant control is applied.

TABLE-IV  
CURRENT THD AND RMS VALUES  
COMPARISON(600RPM,0.95pf)

	Normal (p.u.)	$S_{a1}$ open-circuit fault	The proposed tolerant control
a-	5.4%, 1.51 kA <sub>rms</sub>	14.8%, 1.49 kA <sub>rms</sub>	6.1%, 1.51 kA <sub>rms</sub>
b-	5.4%, 1.51 kA <sub>rms</sub>	9.4%, 1.47 kA <sub>rms</sub>	5.5%, 1.51 kA <sub>rms</sub>
c-	5.4%, 1.51 kA <sub>rms</sub>	8.1%, 1.55 kA <sub>rms</sub>	6.0%, 1.51 kA <sub>rms</sub>

The current THD is increased by the  $S_{a1}$  open-circuit fault; however, owing to the proposed tolerant control, the current THD is restored as good as normal state without any open-circuit fault.

## VI. CONCLUSION

In wind turbine systems consisting of the 5-level converter and the IPMSG, fault-tolerant controls for an open-circuit fault of switches ought to be implemented to improve reliability. This paper proposes a tolerant control for the open-circuit fault of the outer switches in three-level rectifiers (both 5L-NPC and T-type topologies) used in wind turbine systems. A tolerant control for each open-circuit fault is proposed that takes into account the neutral-point voltage balance. This control is implemented by adding a compensation voltage ( $V_{comp}$ ) to the reference voltages for the corresponding compensation ranges depending on the position of the open-circuit fault. The performance and effectiveness of the proposed tolerance control are proved using the simulation results.

## REFERENCES

- [1] A. Isidori, F. M. Rossi, F. Blaabjerg, and K. Ma, "Thermal loading and reliability of 10-MW multilevel wind power converter at different wind roughness classes," *IEEE Trans. Ind. Appl.*, vol. 50, no. 1, pp. 484–494, Jan./Feb. 2014.
- [2] H. G. Jeong, K. B. Lee, S. Chio, and W. Choi, "Performance improvement of LCL-filter-based grid-connected inverters using PQR power transformation," *IEEE Trans. Power Electron.*, vol. 25, no. 5, pp. 1320–1330, May 2010.
- [3] S. Li, T. A. Haskew, R. P. Swatloski, and W. Gathings, "Optimal and direct-current vector control of direct-driven PMSG wind turbines," *IEEE Trans. Power Electron.*, vol. 27, no. 5, pp. 2325–2337, May 2012.
- [4] W. Qiao, L. Qu, and R. G. Harley, "Control of IPM synchronous generator for maximum wind power generation considering magnetic saturation," *IEEE Trans. Ind. Appl.*, vol. 45, no. 3, pp. 1095–1105, May/Jun. 2009.
- [5] S. Morimoto, H. Nakayama, M. Sanada, and Y. Takeda, "Sensor less output maximization control for variable-speed wind generation system using IPMSG," *IEEE Trans. Ind. Appl.*, vol. 41, no. 1, pp. 60–67, Jan./Feb. 2005.
- [6] Y. Zhao, W. Qiao, and L. Wu, "An adaptive quasi-sliding-mode rotor position observer-based sensor less control for interior permanent magnet synchronous machines," *IEEE Trans. Power Electron.*, vol. 28, no. 12, pp. 5618–5629, Dec. 2013.
- [7] P. B. Reddy, A. M. EL-Refaeie, and K. K. Huh, "Effect of number of layers on performance of fractional-slot concentrated-windings interior permanent magnet machines," *IEEE Trans. Power Electron.*, vol. 30, no. 4, pp. 2205–2218, Apr. 2015.
- [8] J. S. Lee and K. B. Lee, "New modulation techniques for a leakage current reduction and a neutral-point voltage balance in transformer less photovoltaic systems using a three-level inverter," *IEEE Trans. Power Electron.*, vol. 29, no. 4, pp. 1720–1732, Apr. 2014.
- [9] U. M. Choi, H. G. Jeong, K. B. Lee, and F. Blaabjerg, "Method for detecting an open-switch fault in a grid-connected NPC inverter system," *IEEE Trans. Power Electron.*, vol. 27, no. 6, pp. 2726–2739, Jun. 2012.
- [10] U. M. Choi, J. S. Lee, and K. B. Lee, "New modulation strategy to balance the neutral-point voltage for three-level neutral-clamped inverter systems," *IEEE Trans. Energy Convers.*, vol. 29, no. 1, pp. 91–100, Mar. 2014.
- [11] M. Schweizer and J. W. Kolar, "Design and implementation of a highly efficient three-level t-type converter for low-voltage applications," *IEEE*

Trans. Power Electron., vol. 28, no. 2, pp. 899–907, Feb. 2013.

[12] U. M. Choi, F. Blaabjerg, and K. B. Lee, “Reliability improvement of a t-type three-level inverter with fault-tolerant control strategy,” IEEE Trans. Power Electron., vol. 30, no. 5, pp. 2660–2673, May 2015.

[13] J. S. Lee and K. B. Lee, “An open-switch fault detection method and tolerance controls based on SVM in a grid-connected t-type rectifier with unity power factor,” IEEE Trans. Ind. Electron., vol. 61, no. 12, pp. 7092–7104, Dec. 2014

[14] H. K. Ku, W. S. Im, J. M. Kim, and Y. S. Suh, “Fault detection and tolerant control of 3-phase NPC active rectifier,” in Proc. IEEE Energy Convers. Congr. Expo., Sep. 2012, pp. 4519–1524.

[15] J. S. Lee, K. B. Lee, and F. Blaabjerg “Open-switch fault detection method of an NPC converter for wind turbine systems,” in Proc. IEEE Energy Convers. Congr. Expo., Sep. 2013, pp. 1696–1701.

[16] S. Ceballos, J. Pou, E. Robles, J. Zaragoza, and J. L. Martín, “Performance evaluation of fault-tolerant neutral-point-clamped converters,” IEEE Trans. Ind. Electron., vol. 57, no. 8, pp. 2709–2718, Aug. 2010.

[17] J. Li, A. Q. Huang, Z. Liang, “Analysis and design of active NPC (ANPC) inverters for fault-tolerant operation of high-power electrical drives,” IEEE Trans. Power Electron., vol. 27, no. 2, pp. 519–533, Feb. 2012.

[18] Y. Song and B. Wang, “Survey on reliability of power electronic systems,” IEEE Trans. Power Electron., vol. 28, no. 1, pp. 591–604, Jan. 2013.

[19] S. Li and L. Xu, “Strategies of fault tolerant operation for three-level PWM inverters,” IEEE Trans. Power Electron., vol. 21, no. 4, pp. 933–940, Jul. 2006.

[20] J. S. Lee, U. M. Choi, and K. B. Lee, “Comparison of tolerance controls for open-switch fault in a grid-connected T-type rectifier,” IEEE Trans. Power Electron., vol. 30, no. 10, pp. 5810–5820, Nov. 2014.



**S. Bala sai** currently he is pursuing M.Tech (EPS) Degree, in the Department of EEE, N.B.K.R.I.S.T, Vidyanagar, SPSR Nellore, AP, India.

#### AUTHORS PROFILE:



**P. Dhana Selvi** has received her B.Tech degree in EEE from periyar university Tamilnadu, and M.Tech Degree from JNTU Anantapur, Andhra Pradesh. presently she is Pursuing P.hD and working as Assistant Professor in Department of EEE, N.B.K.R.I.S.T, Vidyanagar, SPSR Nellore, AP, India.